JOURNAL OF PROPULSION AND POWER
Vol. 24, No. 4, July–August 2008

Ignition of Iron-Coated and Nickel-Coated Aluminum Particles Under Normal- and Reduced-Gravity Conditions

Timothy A. Andrzejak,* Evgeny Shafirovich,† and Arvind Varma‡
Purdue University, West Lafayette, Indiana 47907

DOI: 10.2514/1.34034

In aluminized solid propellants, the use of Al particles coated by certain transition metals may improve engine performance characteristics, owing to decreased agglomeration and lower ignition temperature of the particles. For this application, a detailed knowledge of particle ignition is required. Earlier, we reported the ignition mechanism of single ~2.5-mm Ni-coated Al particles heated by a laser in Ar and CO_2 atmospheres. In the present work, using the same apparatus, we investigate the ignition mechanism of Fe-coated Al particles. The results show that intermetallic reactions contribute to the heating rate upon Al melting at 660°C, but the particles ignite at 1350–1500°C under normal-gravity conditions. The ignition mechanism includes the formation of a solid Fe_2Al_5 phase at the interface between liquid Al and the coating, with subsequent melting of Fe_2Al_5, formation of a solid FeAl layer, and conversion of the Fe coating to a Fe–Al solid solution. Microgravity (10^{-3}–10^{-2} g) experiments with Fe-coated and Ni-coated Al particles were conducted to reduce convection inside the particles, which may influence phase mixing during ignition. In microgravity, both Ni-coated and Fe-coated Al particles ignited at 1250–1400°C. The significantly lower ignition temperature, compared with conventional oxide-coated Al, suggests that Fe-coated and Ni-coated Al particles are promising candidates for propulsion applications.

I. Introduction

THE combustion of aluminum particles coated by a transition metal (e.g., nickel, iron, cobalt, and copper) has been studied to improve Al ignition characteristics [1–6]. This objective is important for aluminized solid rocket propellants in which Al particles tend to agglomerate during propellant burning, resulting in the incomplete combustion of Al and the formation of Al_2O_3 slag inside the engine [7]. Agglomeration is apparently related to the high ignition temperature of Al (~2050°C), causing long particle residence times in the regressing liquid surface layer of the propellant. It has been suggested [1] that upon ignition, Al particles vaporize the surrounding liquid and the entrained gases free the particle from the liquid surface layer. A reduced particle ignition temperature should thus decrease agglomerate size.

The ignition temperature of Ni-coated Al particles is lower by several hundred Kelvin than that of oxide-covered Al particles [4,6]. This is due to the fact that the coating eliminates the natural Al_2O_3 surface layer, which inhibits ignition and allows exothermic intermetallic reactions to accelerate ignition. These reactions are energetic enough to ignite particles in inert atmospheres. Owing to this feature, Ni-coated Al particles have been used to produce nickel aluminides through combustion synthesis techniques [8,9].

For propellant applications, knowledge of the ignition and combustion of single metal-coated Al particles is essential. Electrodynamic levitation studies established [4] that single 30–60-μm Ni-coated Al particles have significantly shorter ignition delay times than Al particles and as little as 3-wt% Ni is needed for the maximum time reduction. The studies, however, could not provide direct measurements of ignition temperatures or any data regarding ignition mechanisms.

We recently developed an apparatus for laser ignition of larger (greater than 1-mm diameter) particles, which allows real-time temperature measurements via a thermocouple attached directly to the particle [10]. The temperature data are synchronized with high-speed digital video to facilitate analysis. Additionally, the apparatus permits reaction products to be collected for subsequent investigation using scanning electron microscopy (SEM) and energy dispersive x-ray spectroscopy (EDX).

This apparatus was used in a previous study [6] on ~2.5-mm Ni-coated Al particles. It was established that particle ignition is independent of atmosphere (Ar or CO_2) and Ni content. The revealed ignition mechanism relies on intermetallic reactions and phase transformations. Analysis of the temperature-vs-time curves showed that 854°C is critical to particle ignition; at this temperature, exothermic intermetallic reactions begin to contribute to particle heating.

The present paper focuses on the ignition of ~2.5-mm Fe-coated Al particles and its comparison with that of Ni-coated Al particles. One motivation for using Fe coatings is that, unlike Ni, Fe is not toxic. In addition, Fe decreases Al agglomeration during propellant burning more effectively than Ni [1]. The ignition mechanism of Fe-coated Al particles, however, is not understood. One problem is that reactions of Al with Fe are much less exothermic than with Ni. For example, formation enthalpies for FeAl and NiAl are −54.4 and −118.5 kJ/mol, respectively [11]. It is thus unclear whether the role of intermetallic reactions in the ignition mechanism of Fe-coated Al particles is as strong as for Ni-coated Al. To investigate the intermetallic reactions and phase transformations during heating/ignition of Fe-coated Al particles is one objective of the present research work.

The second objective is investigation of microgravity effects on the ignition of both Ni- and Fe-coated Al particles. In our previous experiments with single Ni-coated Al particles under normal gravity [6], it was established that, despite the heterogeneous nature of the original particles, the products become well mixed during the ignition process. In large coated particles, such as those used in this study, convection due to the difference in densities of liquid phases can be significant, causing phase mixing (see the Appendix). Microgravity experiments allow one to decrease convection and thus investigate the ignition process under conditions close to those for smaller particles, for which convection is weaker.

Presented as Paper 5646 at the 43rd AIAA/ASME/SAE/ASEE Joint Propulsion Conference and Exhibit, Cincinnati, OH, 8–11 July 2007; received 14 August 2007; revision received 27 February 2008; accepted for publication 17 March 2008.

*Graduate Research Assistant, School of Chemical Engineering, 480 Stadium Mall Drive. Member AIAA.

†Research Scientist, School of Chemical Engineering, 480 Stadium Mall Drive. Senior Member AIAA.

‡R. Games Slayter Distinguished Professor and Head, School of Chemical Engineering, 480 Stadium Mall Drive.

II. Experimental

As previously noted, we used the same apparatus as in our earlier study on combustion of Ni-coated Al particles [6], described in detail elsewhere [10]. Briefly, an infrared CO_2 laser (Synrad, Inc., Firestar t100) was used to ignite single ~2.5-mm particles in a combustion chamber. The laser power was 90 W in all experiments, with the beam diameter being ~5 mm in the particle location. Thermocouple wires (Omega Engineering, Inc., 26%W/74%Re and 5%W/95%Re) were spot-welded onto opposite sides of the particle to support it and to provide real-time temperature measurements. In this configuration, if temperatures in the wire attachment points are equal, the particle materials, as long as they remain electric conductors, do not influence the thermocouple signal, which is determined only by materials of the two attached wires. If the temperatures in the attachment points are different, the thermocouple signal shows the average temperature. In principle, there is also a possibility that during ignition, liquid aluminum may spread over the particle surface and react exothermically with rhenium of the wires. Our experiments show, however, that this event did not occur. According to estimates [6], the static and dynamic errors of temperature measurements did not exceed ±3 and ±1%, respectively. A high-speed digital video camera (Photron Fastcam-1280PCI) recorded the ignition and combustion processes and was synchronized with temperature and laser on/off data. The apparatus also allowed performing quenching experiments in which the laser was powered-down when the particle temperature exceeded a preset threshold value.

The particles used for this research were 2.38-mm Al spheres (Alpha Aesar) coated with Ni or Fe via a cyclic electroplating method [12] (Federal Technology Group). The previous work [6] used samples containing 6, 29, and 58-wt% Ni, for which all three coatings were resilient enough to withstand the stresses imposed during heating and resisted thermocouple detachment. Iron-coated Al particles containing 5, 25, and 56-wt% Fe were prepared, but only the 56-wt% Fe coatings were sufficiently durable to provide temperature measurements over the entire process.

Studies were performed in pure CO_2 and Ar atmospheres. Experiments in CO_2 are important because it is one of the primary oxidizers of Al in solid rocket motors [7,13]. In addition, combustion of coated Al in CO_2 could be used for propulsion on Mars [14]. Experiments in H_2O, another primary oxidizer in solid rocket motors, as well as in O_2 and air, were not possible for technical reasons. Meanwhile, studies in Ar are useful for examining the Al/coating interaction and for materials synthesis applications. Experiments were conducted under pressure 1 atm at room temperature. All reaction products were cross-sectioned and analyzed using SEM (FEI Nova NanoSEM) with a low-vacuum gaseous analytical detector, acceleration voltage of 15 kV, and beam current of 1×10^{-10} A and using EDX (Oxford Instruments INCA 250 EDX system).

For microgravity experiments, the apparatus was mounted onboard NASA's C-9B research aircraft. An externally controlled rotary stage inside the chamber allowed up to five samples to be ignited, before lid reopening. In this way, it was possible to perform a large number of experiments during the flights, which involved 40–60 parabolas, each with a microgravity (10^{-3}–10^{-2} g) duration of 20–25 s.

III. Ignition of Fe-Coated Al Particles in Normal Gravity

A. Experimental Results on Ignition of Fe-Coated Al Particles

Figure 1 shows the temperature-vs-time profiles for 56-wt% Fe particles heated in CO_2 and Ar, for which the laser was active for the entire duration of the shown time frame. The ignition mark in these profiles indicates the point of simultaneous sharp increases in the particle temperature and the particle brightness, determined by synchronizing the thermocouple signal with high-speed (~2000 frames per second) video recording. Throughout this paper, the particle temperature at this point is called the *ignition temperature*.

Note that the combustion temperature of Fe–Al system is relatively low. Thermodynamic calculations using Thermo software [15] show that for initial components at 298 K, the adiabatic combustion temperature of the Fe–Al system is 911°C for a Fe:Al = 1:1 mole ratio and 998°C for a Fe:Al = 1:3 mole ratio (compare with 1638°C for the Ni–Al system). Thus, the ignition temperature shown in Fig. 1 is reached due to external heating of the particle by the laser. Nevertheless, knowledge of the reaction mechanisms at temperatures from the melting point of Al (660°C) to the melting point of Fe (1538°C) is important to understand the ignition process in oxidizing environments of rocket engines, in which the temperature of ignited particles increases up to the Al boiling point (2519°C at 1 atm). Also, the laser power and sizes of particles and thermocouple wires were the same as in the earlier study [6], which allows direct comparison of results for Fe- and Ni-coated particles.

Ignition temperatures, as previously defined, for Fe-coated Al particles in CO_2 and Ar atmospheres were 1412 ± 12 and 1442 ± 9°C, respectively. Note that these values were obtained by averaging several experiments, and the ranges represent the statistically derived 95% confidence intervals for this procedure. As mentioned in Sec. II, the static and dynamic errors could be ±3 and ±1%, respectively (i.e., up to ±4% in total, or ±57°C). Thus, accounting for overlapping ranges, it may be concluded that there is no significant influence of the atmosphere (CO_2 vs Ar) on particle ignition, and the ignition temperatures are in the range of 1350–1500°C. Unfortunately, quantitative analysis of the temperature profiles, including comparison with our results for Ni-coated Al particles [6], was not possible due to uncertainties in particle surface absorptivities (for the laser radiation, a wavelength of 10.3 μm) and their strong temperature dependences. The absorptivity differences also caused offset for the two curves in Fig. 1.

Figures 2 and 3 show several SEM images, along with the qualitative EDX results, obtained from a particle ignited in CO_2. The presence of Fe_2O_3 and a C-rich phase, not detected in Ar atmosphere, indicate CO_2–shell interactions. Figure 2 also shows the following Fe–Al phases: Fe-rich solid solution (labeled as αFe, according to the Al–Fe phase diagram [16] shown in Fig. 4), FeAl, ε phase, $FeAl_2$, Fe_2Al_5, $FeAl_3$, and Al-rich solid solution, in which brighter phases correspond to larger Fe content. It should be noted that the ε phase is not directly observed, because it only exists at temperatures above 1102°C (see Fig. 4); rather, a finely-phase-separated layer containing 40-at.% Fe was detected (see Fig. 3). The compounds formed from the ε phase during cooling could not be conclusively identified using EDX. The weblike Fe-rich phase is too finely dispersed for direct measurement, but is believed to be FeAl. The Fe-lean phase, unidentified in the phase diagram, was found to consist of 35–37-at.% Fe and is distinctly different from the neighboring $FeAl_2$ (see Fig. 3).

Quenching experiments were performed in which particle heating was terminated at 670, 950, 1180, 1250, and 1350°C. SEM images

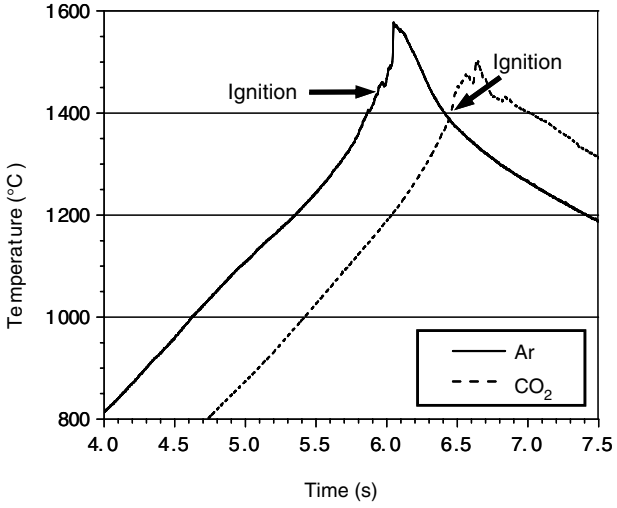

Fig. 1 Typical temperature-vs-time profiles for Fe-coated Al particles ignited in Ar and CO_2 at normal gravity.

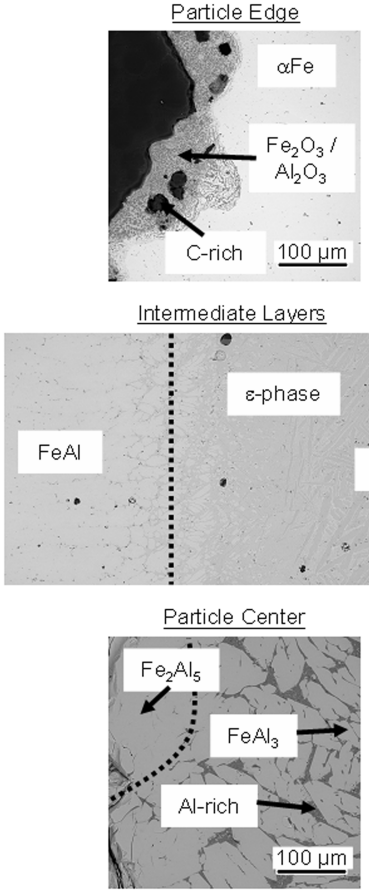

Fig. 2 SEM images of an Fe-coated Al particle ignited in CO_2 atmosphere at normal gravity, displayed with the EDX results.

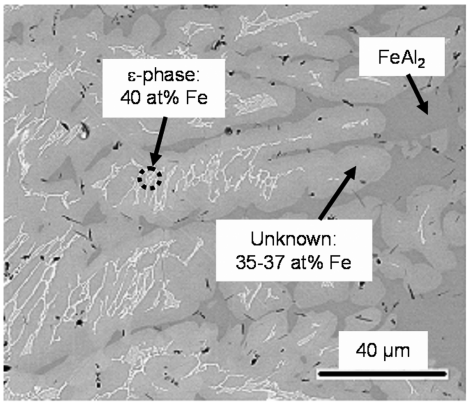

Fig. 3 Magnified SEM image of the separated ε-phase/$FeAl_2$ boundary.

obtained from near the core/shell interface of samples quenched in CO_2 atmosphere are shown in Fig. 5. In contrast to ignited particles, the Fe shell is present in all quenched samples and the Fe-rich solid solution is not detected. For particles quenched at 670 and 950°C, a bilayer of Fe_2Al_5 and $FeAl_3$ exists at the core/shell interface. The preceding multilayer structure is first detected in samples quenched at 1180°C (see Fig. 5c); the layers are thicker in samples in which heating was stopped at 1250 and 1350°C. The same trends concerning the detected Fe–Al compounds were also observed during quenching experiments in Ar atmosphere.

B. Discussion of the Ignition Mechanism for Fe-Coated Al Particles

Comparison of Figs. 2 and 5 indicates that the Fe-rich solid solution (marked as αFe) is detected only after particle ignition. On the other hand, pure Fe is not observed in the postignition products, whereas it remains at the surface of all quenched samples. Thus, it appears that ignition is characterized by the conversion of Fe to a Fe–Al solid solution. This conversion implies that Fe and Al are well mixed, which promotes the reaction, leading to ignition.

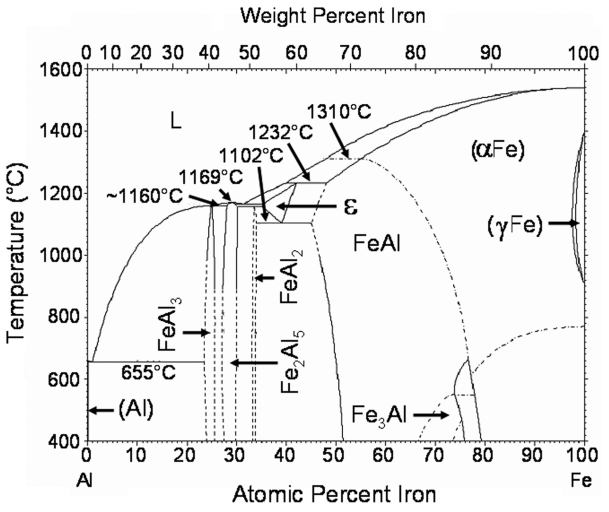

Fig. 4 Aluminum—iron phase diagram [16]; dashed lines represent boundaries that are not well determined.

The preceding SEM/EDX results show that a bilayer of solid $FeAl_3$ and Fe_2Al_5 forms along the core/shell interface of particles quenched at 670 and 950°C (see Figs. 5a and 5b). Because $FeAl_3$ structures are detected in the core region, it is speculated that the $FeAl_3$ present in the bilayer is a result of the precipitation of $FeAl_3$ from solution during particle cooling. At these temperatures, the phase diagram (see Fig. 4) suggests that a single layer of $FeAl_3$ should be present at the interface. The results, however, indicate that Fe_2Al_5 preferentially forms at the interface during particle heating.

In a similar manner, FeAl is detected in particles quenched at 1180°C (see Fig. 5c), despite the phase diagram indicating that the highest-Fe-content phase should be the ε phase. This may be explained by the transient nature of the heating process and the heterogeneous structure of the original particles (insufficient cooling rate may also be a reason). Thus, in this sense, the Fe–Al system differs from the Ni–Al system, in which the ignition mechanism closely followed the (equilibrium) phase diagram [6].

Further, when Fe-coated particles are quenched above the melting point of Fe_2Al_5 (at 1169°C), several layers of Fe–Al compounds are detected (see Figs. 5c–5e). This layered structure consists of (in order from the shell interface inward) FeAl, ε phase, $FeAl_2$, and Fe_2Al_5. In samples quenched at 1350°C (i.e., just before ignition), the majority of the volume consists of the layered structure.

Although 1350°C exceeds the melting points of the layer compounds, mixing does not occur as in the case of Ni-coated Al particles [6]. There is some mild blending of the layers where they meet, but no evidence of mixing exists other than the $FeAl_3$ structures shown in Figs. 2 and 5. For Ni-coated Al particles, complex islands formed, consisting of Ni_2Al_3 surrounded by $NiAl_3$ in an Al-rich phase, which were the result of Ni_2Al_3 first precipitating from the melt, followed by $NiAl_3$ during particle cooling. Because the diffusion rates of Fe and Ni in liquid Al are comparable and convection effects at normal gravity are significant (see the Appendix), the observed difference in phase mixing for particles coated by Fe and Ni is likely due to the significantly different heat effects for the two reaction systems (see Sec. I).

The ignition mechanism for Fe-coated Al particles that has been postulated from the preceding results is as follows:

1) At 660°C, Al melts, allowing the formation of solid Fe_2Al_5 at the interface and Fe dissolution in the core.

2) At 1169°C, Fe_2Al_5 melts, followed by formation of solid FeAl at the interface.

3) At 1350–1500°C, ignition occurs and is related to the conversion of Fe coating into a Fe–Al solid solution.

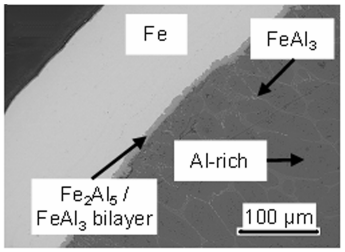

a)

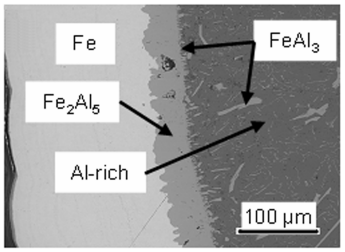

b)

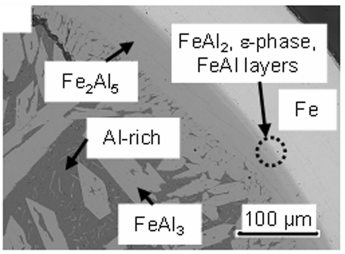

c)

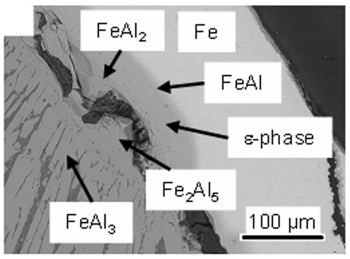

d)

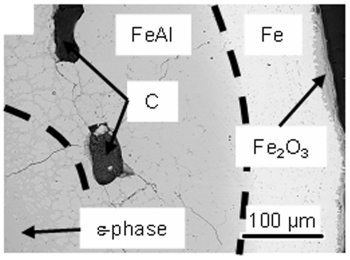

e)

Fig. 5 SEM images (presented with EDX results) of Fe-coated Al particles quenched during heating in CO_2 atmosphere at normal gravity: a) 670°C, b) 950°C, c) 1180°C, d) 1250°C, and e) 1350°C.

The steps of the ignition mechanism are highlighted in Fig. 6, in which the temperature gradient is shown, along with the temperature curve for an Fe-coated Al particle ignited in CO_2. The plot shows that an exothermic reaction causes the measured temperature to rise even during melting of Al near the particle center (step 1). The intermetallic reaction contributes noticeably to particle heating upon completion of Al melting (the heating rate is higher after Al melting than before). At ~1170°C, the slope of the gradient curve increases, indicating transition to step 2 in the ignition mechanism. Finally, a distinct increase in the heating rate is observed at ~1400°C (step 3).

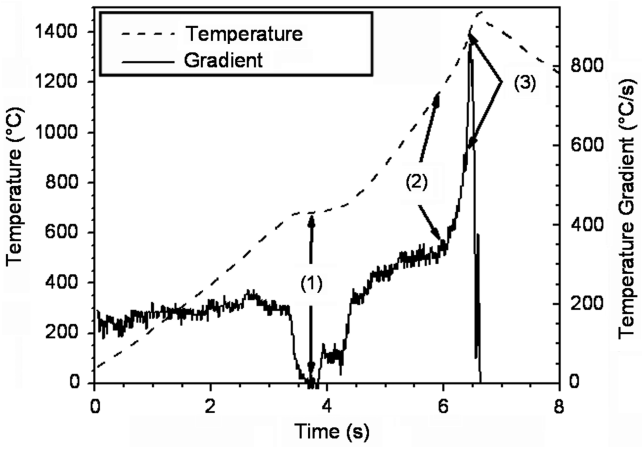

Fig. 6 Typical temperature-vs-time and temperature gradient-vs-time curves for an Fe-coated particle ignited in CO_2 at normal gravity.

An important difference exists between the temperature gradient curves of Fe- and Ni-coated [6] particles. For Ni coatings, intermetallic reactions do not appreciably influence the heating rate until the melting of $NiAl_3$ at 854°C, and as a result, this temperature was determined to be critical for particle ignition. For Fe-coated Al particles, as previously described, reactions contribute significantly to the heating rate upon Al melting at 660°C. The lower temperature required for thermal contributions from intermetallic reactions, compared with Ni-coated particles, may explain the more favorable influence of Fe coatings on agglomeration during propellant combustion, as observed in [1].

IV. Ignition of Ni- and Fe-Coated Al Particles in Microgravity

A. Experimental Results on Ignition of Ni-Coated Al Particles

Figure 7 illustrates that the temperature-vs-time curves from experiments in microgravity are nearly identical to those from normal-gravity studies. As shown in Table 1, the ignition temperatures in micro and normal gravity are statistically inseparable. Note that fewer microgravity experiments were conducted in CO_2 than in Ar, thus increasing the statistical variation. Neglecting the large scatter in this particular case (CO_2 and microgravity) and accounting for potential errors of the temperature measurement technique (see Sec. III.A), we can conclude that the ignition temperatures of Ni-coated Al particles are in the range 1250–1400°C under both normal-gravity and microgravity (10^{-3}–10^{-2} g) conditions.

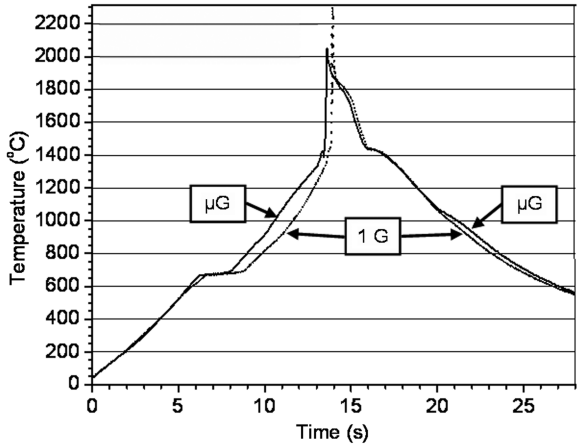

Fig. 7 Typical temperature-vs-time curves for 58-wt% Ni-coated Al particles ignited in CO_2 atmosphere during micro- and normal-gravity experiments.

Table 1 Ignition temperatures for Ni-coated Al particles in micro and normal gravity, with 95% confidence intervals

	Microgravity		Normal gravity	
	58-wt% Ni	29-wt% Ni	58-wt% Ni	29-wt% Ni
Ar	1332 ± 21°C	1309 ± 38°C	1340 ± 37°C	1313 ± 41°C
CO_2	1356 ± 72°C	1327 ± 196°C	1323 ± 20°C	1327 ± 18°C

Figures 8 and 9 represent SEM images of whole sample and core-shell interface regions, respectively, for 29-wt% Ni particles heated in Ar. The EDX analysis (Fig. 9) shows that

1) At 660°C, only Ni_3Al exists at the core/shell interface (as formed by solid-state diffusion before Al melting).

2) At 750°C, an $NiAl_3$ layer is present at the core/shell interface, with finely dispersed $NiAl_3$ in the core region.

3) At 950°C, an Ni_2Al_3 layer is detected at the interface, with larger $NiAl_3$ formations in the core region.

4) At 1150°C, composite $Ni_2Al_3/NiAl_3$ structures are present in the core region.

5) At postignition, phases are well mixed, consisting of finely dispersed $Ni_2Al_3/NiAl_3$ structures in an Al-rich phase.

The phase diagram (Fig. 10) is helpful to understand the preceding sequence of events. In particular, the melting points of Al, $NiAl_3$, and Ni_2Al_3 are 660, 854, and 1133°C, respectively. It should be noted that the satellite regions in Figs. 8b and 8c represent Al beads that formed owing to thermal stresses cracking the Ni shell [6]. The brightest regions in Fig. 8e are the thermocouple wires embedded in the particle after ignition. For 58-wt% Ni, features for all quenched samples were similar to the 29-wt% Ni samples, whereas, in contrast, the ignited samples were predominantly Ni_2Al_3. It is remarkable that the SEM/EDX results were qualitatively the same for micro- and normal-gravity environments.

An interesting result from normal-gravity experiments, not reported previously in [6], is that particle self-ignition after laser heating is stopped at temperatures as low as 1150°C. The same phenomenon, however, does not occur during experiments in microgravity (Fig. 11).

B. Experimental Results on Ignition of Fe-Coated Al Particles

Figure 12 demonstrates typical temperature-vs-time curves from micro- and normal-gravity experiments in CO_2 atmosphere. Analysis of such curves shows (see Table 2) that ignition temperature is independent of atmosphere (Ar or CO_2) and lower in the microgravity environment. In light of potential temperature measurement errors, we can conclude that the ignition temperatures of Fe-coated Al particles under microgravity (10^{-3}–10^{-2} g) conditions are in the range of 1250–1400°C (i.e., the same as for Ni-coated Al particles).

SEM images of particles heated in CO_2 are presented in Figs. 13 and 14, in which whole sample and magnified core/shell interface images are shown, respectively. The EDX analysis (Fig. 14) shows that

1) At 660°C, Fe_2Al_5 is present at the core/shell interface.

2) At 750°C, fine weblike $FeAl_3$ structures form in the core region.

3) At 1180°C, thin layers of FeAl, ε phase, and $FeAl_2$ are detected at the interface; larger structures of $FeAl_3$ dispersed in an Al-rich phase are also present.

4) At 1320°C, layers are thicker, and Fe_2O_3 is present on the shell surface.

5) Postignition, a multilayered structure is present, where, following the Fe–Al phase diagram (Fig. 4), αFe indicates Fe-rich solid solution.

As shown in Fig. 13, Fe is only detected before ignition, whereas the Fe-rich solid solution is present only after ignition. Note that nearly all the compounds/phases in the Fe–Al phase diagram (Fig. 4) were detected in the postignition products. Features of the phase diagram of particular interest are the melting points of Al, Fe_2Al_5, and FeAl at 660, 1169, and 1310°C, respectively. The SEM/EDX results are qualitatively the same as in normal-gravity experiments.

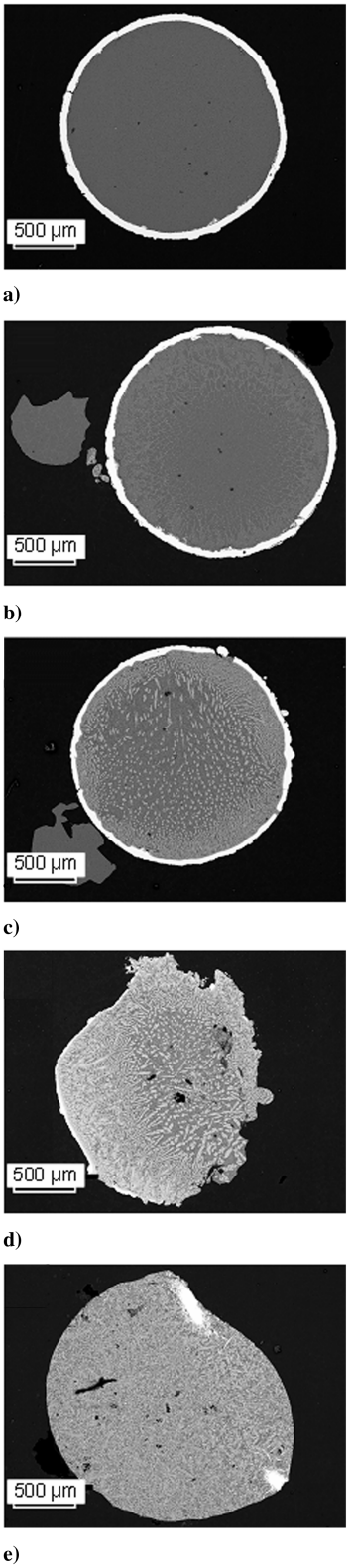

Fig. 8 Whole sample SEM images of 29-wt% Ni particles heated in Ar atmosphere during microgravity, quenched at a) 660°C, b) 750°C, c) 950°C, d) 1150°C, and e) ignited.

C. Discussion of Microgravity Effects on Ignition Mechanisms of Ni- and Fe-Coated Al Particles

Figure 8 clearly illustrates the transport of Ni from the shell to the center of the Ni-coated Al particle as temperature increases in microgravity. As previously noted, the EDX results were essentially the same as those obtained from experiments in normal gravity [6]. This similarity indicates that the buoyancy variation does not

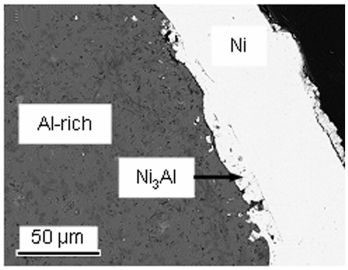

a)

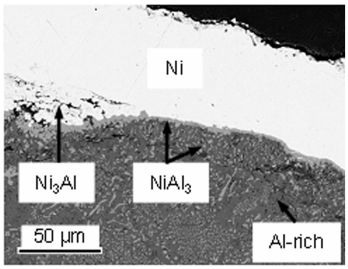

b)

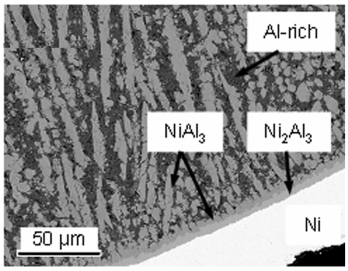

c)

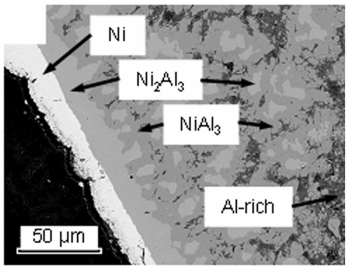

d)

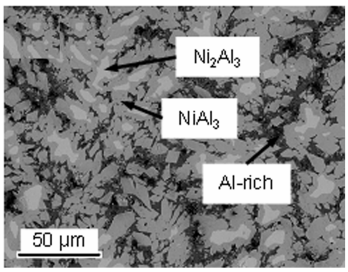

e)

Fig. 9 Magnified SEM images of 29-wt% Ni particles heated in Ar atmosphere during microgravity, quenched at a) 660°C, b) 750°C, c) 950°C, d) 1150°C, and e) ignited. The ignited particle image shows phases in the particle center.

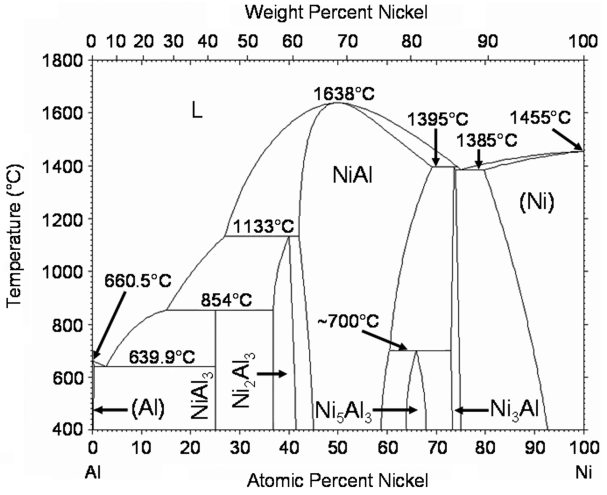

Fig. 10 Nickel—aluminum phase diagram [16].

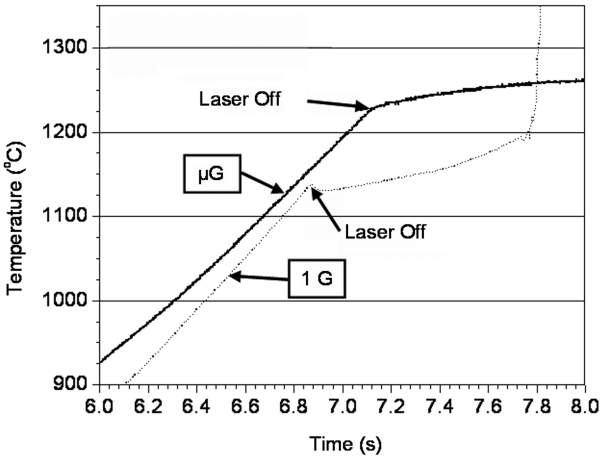

Fig. 11 Temperature-vs-time curves for 29-wt% Ni-coated Al particles heated in Ar during micro- and normal-gravity experiments; the laser was turned off before reaching ignition temperature.

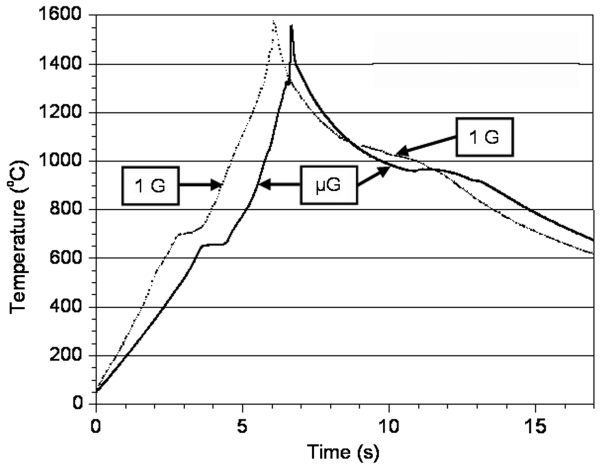

Fig. 12 Typical temperature-vs-time curves for 56-wt% Fe particles ignited in CO_2 atmosphere during micro and normal gravity.

significantly influence ignition, provided the particle is undergoing constant external heating (the self-heating results will be discussed later).

For Fe-coated Al particles, the SEM images (Figs. 13 and 14) also do not display qualitative differences from those obtained during normal-gravity experiments (Figs. 2, 3, and 5). A delay, however, was detected in the extent of formation of the Fe–Al compound layers, as highlighted in Fig. 15, in which SEM images of particles quenched at 1250°C in micro and normal gravity are presented. These observations indicate that, in contrast to the Ni–Al system, mixing in the liquid core is influenced by the buoyancy difference.

For Ni-coated Al particles, no detectable difference was observed in the ignition temperatures and temperature-vs-time profiles

Table 2 Ignition temperatures for 56-wt% Fe-coated Al particles in micro and normal gravity, with 95% confidence intervals

	Microgravity	Normal gravity
Ar	1304 ± 33°C	1442 ± 9°C
CO_2	1317 ± 30°C	1412 ± 12°C

obtained in microgravity, compared with normal-gravity results (see Fig. 6 and Table 1). This suggests that despite the lesser influence of buoyancy, the reactions at the interface proceed in the same manner as in normal gravity.

For Fe-coated Al particles, however, microgravity experiments indicated that ignition temperatures were lower than those obtained in normal gravity (see Table 2). This effect may be explained as follows. As shown in Sec. III, the last stage in the ignition mechanism of Fe-coated Al particles is associated with conversion of Fe to a Fe-rich solid solution. According to the phase diagram (Fig. 4), the formation of this solid solution from the melt is possible at temperatures higher than 1310°C. It appears from the measured ignition temperatures (see Table 2) that, in microgravity, sufficient melt concentrations of Fe exist near the particle-shell interface at ~1310°C to initiate the formation of Fe–Al solid solution, thus causing ignition. In normal gravity, the stronger buoyancy effects may decrease Fe melt concentration over a large fraction of the shell interface, thus elevating the ignition temperature. It appears that the concomitant increase of Fe concentration at the bottom part of the particle is unable to compensate for this effect.

Figure 11 shows that for Ni-coated Al particles, self-heating initiates ignition under normal-gravity conditions, but not in microgravity, even though the laser was turned off at higher temperature. This indicates that higher buoyancy effects are required for the particle self-ignition phenomenon.

Figure 11 also shows a reduced ignition temperature (1190°C), compared with the observations during constant-heating experiments. The SEM/EDX analyses of quenched samples reveal that the formation of NiAl locally erodes the Ni shell, and this phenomenon was more pronounced in normal gravity (Fig. 16). Apparently, buoyancy mixing provides the Al needed for the NiAl formation to propagate through the shell. As the NiAl penetrates deeper into the shell, the reaction surface area becomes larger, which increases the reaction rate. This is in agreement with the observed acceleration in particle heating rate just before ignition occurs. Because ignition of Ni-coated Al particles is affected by the balance between reaction heat release and heat loss [6], the described increase in reaction rate lowers the ignition temperature. Note that self-ignition was not observed for the Fe–Al system, in agreement with the lower adiabatic combustion temperature for this system (see Sec. III.A).

Because 1–100 μm Al particles are typically used in propulsion applications, the applicability of the results obtained for ~2.5-mm particles in this study is an important question. The described microgravity experiments were conducted at 10^{-3}–10^{-2} g. According to the Grashof criterion (see the Appendix), the same decrease of convection would occur for 250–550-μm-diam particles in normal gravity. It should be noted that experiments with 2.5-mm particles at 10^{-6} g would simulate convection in 25-μm particles at 1 g. Unfortunately, the microgravity level 10^{-6} g and relatively long experimental time required (greater than 10 s) can be achieved only in space flight.

Although microgravity decreases buoyancy effects, some other problems in extrapolation of the obtained results to smaller particle sizes still remain. As shown in the SEM images, some layer thicknesses and grain sizes are comparable with the practical particle size range. Similarly, the heating rates in the conducted experiments were significantly lower than those in applications; the effects of heating rate on the combustion of Ni–Al system have been demonstrated experimentally [3,9] and theoretically [17]. Thus, a direct application of the obtained results to smaller particles is difficult. Note, however, that for Ni-coated Al particles, a significant (by several hundred Kelvin) decrease in the ignition temperature, compared with conventional oxide-coated Al particles, was observed

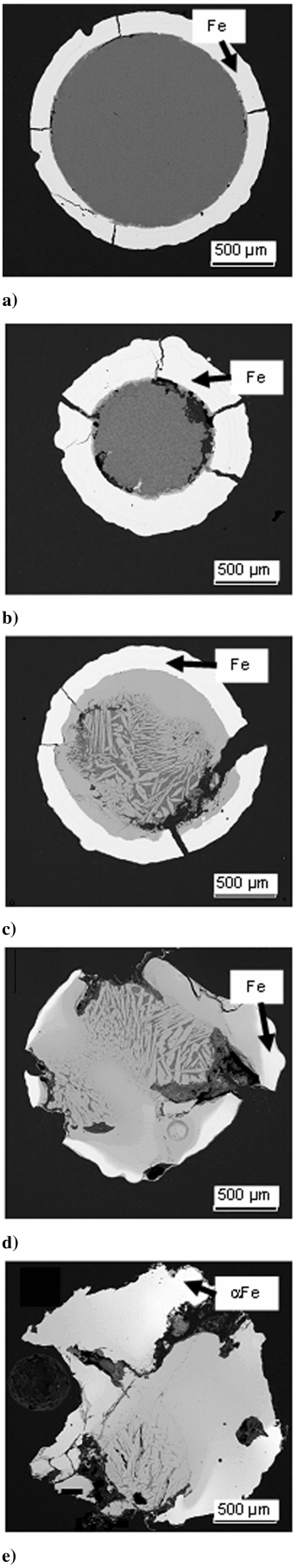

Fig. 13 Whole sample SEM images of 56-wt% Fe particles heated in CO_2 atmosphere during microgravity, quenched at a) 660°C, b) 750°C, c) 1180°C, d) 1320°C, and e) ignited.

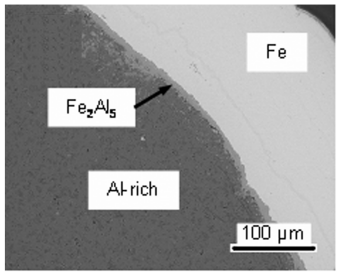

a)

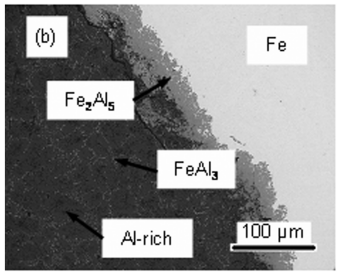

b)

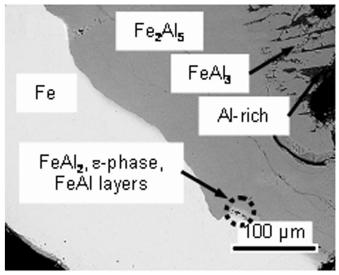

c)

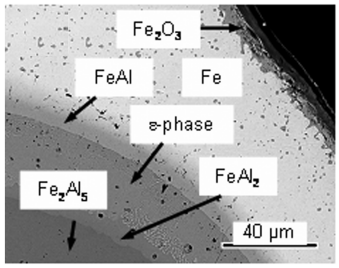

d)

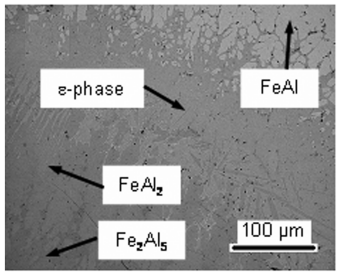

e)

Fig. 14 Magnified SEM images of 56-wt% Fe particles heated in CO_2 atmosphere during microgravity, quenched at a) 660°C, b) 750°C, c) 1180°C, d) 1320°C, and e) ignited (away from edge region).

in studies with both smaller [4] and larger [6] particles. Thus, it is expected that a similar decrease in the ignition temperature will be observed for smaller Fe-coated Al particles.

V. Conclusions

The ignition mechanism for 2.5-mm Fe-coated Al particles, heated by an infrared laser in Ar and CO_2 environments, includes the formation of Fe_2Al_5 at the shell/core interface at 660°C, followed by the appearance of FeAl at 1169°C. Ignition is related to the conversion of the Fe coating to a Fe–Al solid solution, and in normal gravity, it occurs at 1350–1500°C for both Ar and CO_2 atmospheres. The postignition products for Fe-coated particles are not well mixed and contain layers of different Fe–Al compounds.

The ignition temperatures of 2.5-mm Ni-coated Al particles under constant laser heating are similar in micro and normal gravity, 1250–1400°C, and are also independent of the ambient atmosphere (Ar or CO_2). The buoyancy difference is not negligible, however, as shown by the influence of gravity on particle self-ignition. The ignition temperatures of Fe-coated Al particles in microgravity are in the

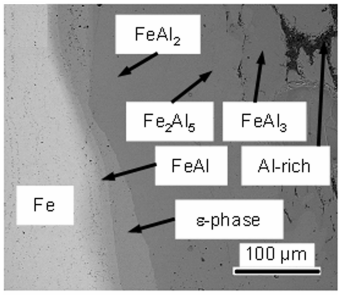

a)

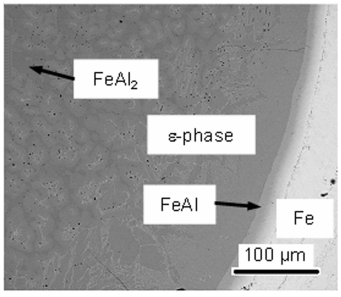

b)

Fig. 15 SEM images of 56-wt% Fe particles quenched at 1250°C in Ar atmosphere during a) micro and b) normal gravity.

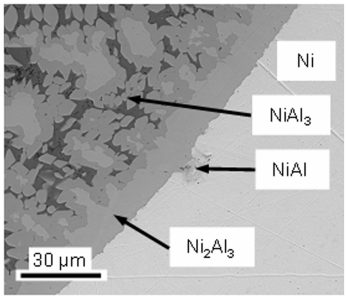

a)

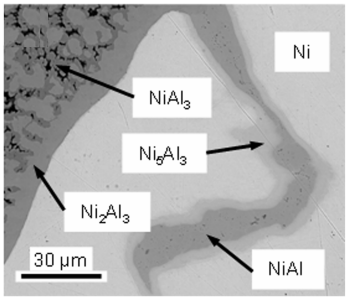

b)

Fig. 16 Penetration by NiAl into the shell for particles quenched at 1200°C during a) micro and b) normal gravity.

same range as for Ni-coated Al particles. The significantly lower ignition temperature, compared with conventional oxide-coated Al (~2050°C), suggests that both Fe-coated and Ni-coated Al particles are promising candidates for propulsion applications.

Appendix: Estimates of Intraparticle Diffusion and Convection

The diffusivity of Ni in liquid Al can be determined by the following formula:

$$D = D_0 \cdot \exp\left(-\frac{E_a}{RT}\right) \tag{A1}$$

where D_0 and E_a, obtained at temperatures of 900–1100°C, are 4.8×10^{-6} m^2/s and 74.9 ± 12.1 kJ/mol, respectively [18]. According to [18], these parameters remain valid over the temperature range between the melting points of Al (660°C) and the product (1638°C for NiAl). Thus, for example, at 1600°C, the Ni–Al diffusivity is 3.9×10^{-8} m^2/s. The characteristic time of diffusion is estimated by the following relation:

$$t_d = \frac{L^2}{D} \tag{A2}$$

where L is the characteristic length. Assuming that L is the radius of the Al core (1.19 mm), $t_d = 36$ s. Because this period is longer than the experimental heating times (4–8 s from Al melting to particle ignition) [6], the observed good mixing cannot be explained by diffusion.

The diffusivity of Al in liquid Fe (melting point of 1538°C) at temperatures of 1550–1650°C is given by Equation (A1), where D_0 and E_a are $(1.0 \pm 0.11) \times 10^{-6}$ m^2/s and 81.5 kJ/mol, respectively [19]. At the same temperature (1600°C) as in the preceding estimate, the diffusivity of Al in Fe is 0.53×10^{-8} m^2/s. The used parameters [19], however, were obtained for 1.4-mass% Al; it was reported that with increasing Al mass fraction, the diffusivity increases several fold. Thus, it may be concluded that the diffusivity and hence the characteristic time of diffusion in Fe-coated Al particles are of the same order of magnitude as for Ni-coated Al particles.

The Grashof number for convection (buoyancy), resulting from variation in fluid density, can be estimated by

$$Gr = \frac{(\rho_1 - \rho_2) \cdot g \cdot L^3}{\rho \cdot \nu^2} \tag{A3}$$

where ρ_1 and ρ_2 are the densities of liquid phases ($\rho_1 > \rho_2$), ρ is the average density, ν is the average kinematic viscosity, and g is the gravitational acceleration. For Ni-coated Al particles, using density and viscosity data from [11], $\rho_1 = 7686$ kg/m^3 (liquid Ni), $\rho_2 = 2043$ kg/m^3 (liquid Al), $\rho = 4865$ kg/m^3, $\nu = 3.580 \times 10^{-7}$ m^2/s, $g = 9.807$ m/s^2, and Eq. (A3) yields $Gr = 1.50 \times 10^5$. This high value for Gr indicates that well-developed convection may occur, resulting in faster phase mixing than diffusion. For Fe-coated Al particles, Gr estimate by Eq. (A3) leads to the same conclusion.

Acknowledgments

This work was funded by NASA grant NNC04AA36A, with Paul Ferkul serving as the Technical Monitor. The authors thank David G. Taylor for assistance in development of the experimental setup.

References

[1] Breiter, A. L., Mal'tsev, V. M., and Popov, E. I., "Means of Modifying Metallic Fuel in Condensed Systems," *Combustion, Explosion, and Shock Waves*, Vol. 26, No. 1, 1990, pp. 86–92. doi:10.1007/BF00742280

[2] Yagodnikov, D. A., and Voronetskii, A. V., "Experimental and Theoretical Study of the Ignition and Combustion of an Aerosol of Encapsulated Aluminum Particles," *Combustion, Explosion, and Shock Waves*, Vol. 33, No. 1, 1997, pp. 49–55. doi:10.1007/BF02671852

[3] Shafirovich, E., Mukasyan, A., Thiers, L., Varma, A., Legrand, B., Chauveau, C., and Gökalp, I., "Ignition and Combustion of Al Particles Clad by Ni," *Combustion Science and Technology*, Vol. 174, No. 3, 2002, pp. 125–140. doi:10.1080/713712997

[4] Shafirovich, E., Escot Bocanegra, P., Chauveau, C., Gökalp, I., Goldshleger, U., Rosenband, V., and Gany, A., "Ignition of Single Nickel-Coated Aluminum Particles," *Proceedings of the Combustion Institute*, Vol. 30, Combustion Inst., Pittsburgh, PA, 2005, pp. 2055–2062. doi:10.1016/j.proci.2004.08.107

[5] Hahma, A., Gany, A., and Palovuori, K., "Combustion of Activated Aluminum," *Combustion and Flame*, Vol. 145, No. 3, 2006, pp. 464–480. doi:10.1016/j.combustflame.2006.01.003

[6] Andrzejak, T. A., Shafirovich, E., and Varma, A., "Ignition Mechanism of Nickel-Coated Aluminum Particles," *Combustion and Flame*, Vol. 150, Nos. 1–2, 2007, pp. 60–70. doi:10.1016/j.combustflame.2007.03.004

[7] Price, E. W., and Sigman, R. K., "Combustion of Aluminized Solid Propellants," In: *Solid Propellant Chemistry, Combustion and Motor Ballistics*, edited by V. Yang, T. B. Brill and, W. Z. Ren, Vol. 185, Progress in Astronautics and Aeronautics, AIAA, Reston, VA, 2000, pp. 663–685.

[8] Mukasyan, A. S., Lau, C., and Varma, A., "Gasless Combustion of Aluminum Particles Clad by Nickel," *Combustion Science and Technology*, Vol. 170, No. 1, 2001, pp. 67–85. doi:10.1080/00102200108907850

[9] Thiers, L., Mukasyan, A. S., and Varma, A., "Thermal Explosion in Ni–Al System: Influence of Reaction Medium Microstructure," *Combustion and Flame*, Vol. 131, Nos. 1–2, 2002, pp. 198–209. doi:10.1016/S0010-2180(02)00402-9

[10] Andrzejak, T. A., Shafirovich, E., Taylor, D. G., and Varma, A., "Apparatus for Studies of High-Temperature Chemical Reactions in Single Particle Systems," *Review of Scientific Instruments*, Vol. 78, No. 8, 2007, Paper 085102. doi:10.1063/1.2760861

[11] Gale, W. F., and Totemeier, T. C. (eds.), *Smithells Metals Reference Book*, 8th ed., Butterworth–Heinemann, Oxford, 2004.

[12] Yih, P., "Method for Electroplating Metal Coating(s) Particulates at High Coating Speed with High Current Density," U.S. Patent 6,010,610, issued 4 Jan. 2000.

[13] Bazyn, T., Krier, H., and Glumac, N., "Oxidizer and Pressure Effects on the Combustion of 10-μm Aluminum Particles," *Journal of Propulsion and Power*, Vol. 21, No. 4, 2005, pp. 577–582. doi:10.2514/1.12732

[14] Shafirovich, E., and Varma, A., "Metal-CO_2 Propulsion for Mars Missions: Current Status and Opportunities," *Journal of Propulsion and Power*, Vol. 208, No. 3, 2008, pp. 385–394. doi:10.2514/1.32635

[15] Shiryaev, A. A., "Thermodynamics of SHS Processes: An Advanced Approach," *International Journal of Self-Propagating High-Temperature Synthesis*, Vol. 4, No. 4, 1995, pp. 351–362.

[16] Massalski, T. B. (ed.), *Binary Alloy Phase Diagrams*, 2nd ed., ASM International, Materials Park, OH, 1990.

[17] Khina, B. B., "Modeling Nonisothermal Interaction Kinetics in the Condensed State: A Diagram of Phase Formation Mechanisms for the Ni–Al system," *Journal of Applied Physics*, Vol. 101, No. 6, 2007, Paper 063510. doi:10.1063/1.2710443

[18] Naiborodenko, Yu. S., and Itin, V. I., "Gasless Combustion of Metal Powder Mixtures 1: Mechanism and Details," *Combustion, Explosion and Shock Waves*, Vol. 11, No. 3, 1975, pp. 293–300. doi:10.1007/BF00740533

[19] Kawakami, M., Yokoyama, S., Takagi, K., Nishimura, M., and Kim, J.-S., "Effect of Aluminum and Oxygen Content on Diffusivity of Aluminum in Molten Iron," *Iron and Steel Institute of Japan International*, Vol. 37, No. 5, 1997, pp. 425–431. doi:10.2355/isijinternational.37.425

C. Avedisian
Associate Editor